

High Wall Stress May Predict the Formation of Stent-Graft–Induced New Entries After Thoracic Endovascular Aortic Repair

Claudia Menichini, PhD¹, Selene Pirola, MSc¹, Baolei Guo, PhD², Weiguo Fu, MD², Zhihui Dong, MD, PhD², and Xiao Yun Xu, PhD¹

¹Department of Chemical Engineering, Imperial College London, UK

²Department of Vascular Surgery, Zhongshan Hospital, and Institute of Vascular Surgery, Fudan University, Shanghai, China

Corresponding Authors:

Professor Xiao Yun Xu, Department of Chemical Engineering, Imperial College London, London SW7 2AZ, UK. Email: yun.xu@imperial.ac.uk

Dr Zhihui Dong, Department of Vascular Surgery, Zhongshan Hospital, and Institute of Vascular Surgery, Fudan University, 180 Fenglin Road, Shanghai 200032, China. Email: dong.zhihui@zs-hospital.sh.cn

Abstract

Purpose: To explore the potential role of morphological factors and wall stress in the formation of stent-graft–induced new entries (SINE) based on computed tomography (CT) images after thoracic endovascular aortic repair (TEVAR).

Case Report: Two female patients aged 59 (Patient 1) and 44 (Patient 2) years underwent TEVAR for type B dissection in the chronic (Patient 1) or subacute (Patient 2) phase. CT scans at 3-month follow-up showed varying degrees of false lumen thrombosis in both patients. At 14-month follow-up, a SINE was observed in Patient 1 while the dissected aorta in the other patient remained stable. Morphological and finite element analyses were performed based on the first follow-up CT images. The computational results showed that the SINE patient had higher stent-graft tortuosity than the non-SINE patient and much higher wall stress in the region close to the distal SINE.

Conclusions: This case study shows that high stent-graft tortuosity can lead to high wall stress, which is potentially linked to the formation of SINE. Further large population-based studies are needed to confirm this preliminary finding.

Keywords

Aortic dissection, finite element analysis, new entry tears, stent-graft, stent-graft–induced new entries, thoracic endovascular aortic repair, type B dissection, wall stress

Introduction

The formation of stent-graft–induced new entries (SINE) is a potentially life-threatening complication that can arise after thoracic endovascular aortic repair (TEVAR) in Stanford type B dissection patients.^{1,2} This can cause retrograde dissection, pressurization of the false lumen (FL) leading to aneurysm expansion, and/or the formation of a second FL. Stent-graft oversizing, spring-back force (the inherent tendency of stents to return to their initial straight configuration), and pathological fragility of the aortic wall are considered among the main risk factors associated with the formation of SINE.³ Nonetheless, it is still unclear how these factors may affect patient prognosis and which patients would be at high risk to develop SINE after TEVAR.

The objective of this pilot study is to investigate the roles of morphological features and aortic wall stress distribution in the formation of SINE. Stress predictions obtained through finite element analysis are compared between SINE and non-SINE patients to identify potential predictors of SINE formation.

Case Report

Patient-Specific Data

With approval of the Ethics committee of Zhongshan Hospital (affiliated with Fudan University, Shanghai, China; approval no. Y2017-056), anonymized clinical and morphological data from computed tomography (CT) scans were obtained from 2 female patients aged 59 (Patient 1) and 44 (Patient 2) years who underwent TEVAR for type B dissection in the chronic (Patient 1) or subacute (Patient 2) phase. Doppler wire pressure measurements were taken before and immediately after stent-grafting at the time of TEVAR. Both patients gave written informed consent to the CT scans, the TEVAR procedure, and the Doppler wire measurements.

Both patients presented aneurysmal dilatation in the thoracic FL, more pronounced in Patient 1. They were treated with Valiant Captivia stent-grafts (Medtronic, Minneapolis, MN, USA; Patient 1 32×200 mm and Patient 2 28×150 mm). The initial distal stent-graft oversizing (DSO) rates, defined as the ratio of the stent-graft diameter to the pre-TEVAR distal true lumen (TL) diameter, were 101.3% for Patient 1 and 83.0% for Patient 2. In both patients, the thoracic FL appeared almost completely thrombosed

at the first follow-up CT at 3 months after TEVAR, with thrombus formation extending up to the celiac trunk in Patient 1 and to just below the distal end of the stent in Patient 2. The DSO was reduced to 68.2% for Patient 1 and 64.9% for Patient 2 due to the increase in TL volume after stent deployment, indicating the existence of a persistent radial force acting on the aortic wall and dissection flap. At 14 months after TEVAR, a SINE was observed in Patient 1 near the distal end of the stent-graft, which led to aneurysmal growth and the formation of a second FL. The condition of the dissected aorta in Patient 2 remained stable, with no significant changes in FL volume. Both patients were kept under CT surveillance.

Anatomical Measurements

Pre- and post-TEVAR geometries were reconstructed from the corresponding CT images using Mimics software (Materialise HQ, Leuven, Belgium). Key geometrical parameters were measured, including inlet, arch and maximum diameters, length of the thoracic aorta (measured from the centerline), and the tortuosity index (the ratio of the actual length of the measured aortic segment to the straight line distance between the beginning and end of the segment⁴). The tortuosity index was calculated for the thoracic segment, the entire aorta, and the stented segment. TL and FL volumes were calculated based on segmented lumen area and slice thickness.

The reconstructed patient-specific geometries are shown in Figure 1, and all the geometrical measurements are summarized in Table 1. Compared to the non-SINE patient, the SINE patient had a wider aortic arch and a longer and more tortuous aorta, especially in the stent region (>28%).

Structural Analysis

Wall models were built based on the first post-TEVAR follow-up scans with a thickness of 1.4 mm for the aortic wall⁵ and 2.3 mm for the composite stent-wall region.⁶ The aorta and stent-graft were treated as linear elastic materials with Young's moduli of 2 MPa and 8.4 MPa,⁶ respectively. Three uniform static pressure loads were tested: 50 mm Hg (the pulse pressure of Patient 1), 42 mm Hg (the pulse pressure of Patient 2), and 46

mm Hg (the average value). Finite element structural simulations were performed with the Ansys Static Structural solver (Ansys Inc., Canonsburg, PA, USA).

Predicted wall displacements are shown in Figure 2. In both patients, large displacements were observed in the descending aorta and, in particular, just below the stent-graft. Patient 1 had much larger displacements than Patient 2, with values up to 3 mm near the distal end of the stent-graft, proximally to the location of the SINE. The stent-graft itself was also subject to large displacement in its central region.

In addition, high shear strains were observed before the proximal end of the stent-graft and in the descending aorta. While in Patient 2 the largest shear strain was located just above the celiac trunk, in Patient 1 the largest shear strains were observed near the distal end of the stent-graft, proximally to the location of the SINE and aneurysmal dilation.

The predicted wall stress distributions are shown in Figure 3. In both cases and for all loads tested, high stress values were found near the proximal and distal ends of the stent-graft. The peak stress was located near the distal end of the stent-graft in both patients, but Patient 1 had peak values >350 kPa, which were >100 kPa higher (+73%) than in Patient 2.

Discussion

The implantation of a stent-graft brings about changes in the biomechanical properties of the stented thoracic aorta, and the compliance mismatch between the stented and non-stented regions can have consequences on stress and strain distributions.⁷ Also, patient-specific anatomical features can play an important role in determining stress distribution and the location at high risk of tear formation. In this case study, a much wider arch and a longer and more tortuous aorta was observed in the SINE patient (Patient 1), especially in the stent region. These factors had repercussions for stress distribution. Patient 1 had considerably higher stress, with values >350 kPa concentrated near the distal end of the stent-graft. Peak stresses in the range of 290 to 450 kPa have been reported for aneurysmal aortas.⁸ The high stress level found here can be attributed to the mismatch in biomechanical properties between the bare wall and the stent-graft–wall composite and to the different locations of the curving point of

the stent-graft. The latter appears to be close to the proximal region of the stent-graft in Patient 2 while at the middle to distal portion of the stent-graft in Patient 1. This could cause the spring-back force to concentrate near the distal end of the stent-graft in Patient 1, close to the curving point.¹

The higher tortuosity index is also reflected in larger displacement of the stent-graft itself, while large shear strain was observed in the descending aorta just below the device and proximally to the SINE location, causing the descending aortic wall to twist. These results indicated the existence of torsional forces acting on the wall near the distal end of the stent-graft, proximally to the location of SINE. All these factors pointed to an increased risk for wall rupture and SINE formation in Patient 1.

Conclusion

This case study suggests that there is a potential link between high wall stress and the formation of SINE. Finite element analysis based on the first follow-up scans indicated considerably higher stress, torsional strain, and wall displacement in the patient who developed SINE at 14-month follow-up than in the non-SINE patient. Furthermore, the region of high stress and displacement corresponded well with the location of SINE. These preliminary findings suggest that anatomical features such as tortuosity, curvature, and thoracic aortic length may have a strong influence on stress distribution. These factors could act together to cause high stress concentration in a specific area, thereby increasing the risk of SINE formation in this region. Further large population-based studies are needed to confirm these findings.

Declaration of Conflicting Interests

The author(s) declare no potential conflicts of interest with respect to the research, authorship, and/or publication of this article.

Funding

The author(s) report receiving the following financial support for the research, authorship, and/or publication of this article: This work was supported by the

Department of Chemical Engineering at Imperial College London; the Imperial College Healthcare Charity; International Exchange Scheme–Cost Share Programme (2016) between the Royal Society (UK) and NSFC (China) (No. IE161052); the National Natural Science Foundation of China (No. 81371648, No. 81470573, No. 81770474, and No. 81770508); and the International Cooperation Program sponsored by the Science and Technology Committee of Shanghai Municipality (No. 16410722900). Additionally, Selene Pirola is supported by the European Commission within the Horizon 2020 Framework through the MSCA-ITN-ETN European Training Networks (project number 642458).

References

1. Dong Z, Fu W, Wang Y, et al. Stent graft-induced new entry after endovascular repair for Stanford type B aortic dissection. *J Vasc Surg.* 2010;52:1450-1457.
2. Pantaleo A, Jafrancesco G, Buia F, et al. Distal stent graft-induced new entry: an emerging complication of endovascular treatment in aortic dissection. *Ann Thorac Surg* 2016;102:527-532.
3. Jang H, Kim MD, Kim GM, et al. Risk factors for stent graft-induced new entry after thoracic endovascular aortic repair for Stanford type B aortic dissection. *J Vasc Surg* 2017;65:676-685.
4. Shirali AS, Bischoff MS, Lin HM, et al. Predicting the risk for acute type B aortic dissection in hypertensive patients using anatomic variables. *JACC Cardiovasc Imaging.* 2013;6:349-357.
5. Van Puyvelde J, Verbeken E, Verbrugghe P, et al. Aortic wall thickness in patients with ascending aortic aneurysm versus acute aortic dissection. *Eur J Cardio-Thorac.* 2015;49:756-762.
6. Pasta S, Cho J-S, Dur O, et al. Computer modeling for the prediction of thoracic aortic stent graft collapse. *J Vasc Surg.* 2013;57:1353-1361.
7. Rinaudo A, Raffa GM, Scardulla F, et al. Biomechanical implications of excessive endograft protrusion into the aortic arch after thoracic endovascular repair. *Comput Bio Med.* 2015;66:235-241.
8. Vorp DA, Geest JPV. Biomechanical determinants of abdominal aortic aneurysm rupture. *Arterioscler Thromb Vasc Biol.* 2005;25:1558-1566.

Legends

Figure 1. Patient-specific geometries reconstructed from preprocedure and 3-month follow-up data, as well as after 1 year (Patient 2) and 14 months (Patient 1).



Figure 2. (A) Total displacements with vectors and (B) shear strain in the XY direction in Patients 1 and 2 obtained with the highest pressure load tested (50 mm Hg), corresponding to the pulse pressure in Patient 1.

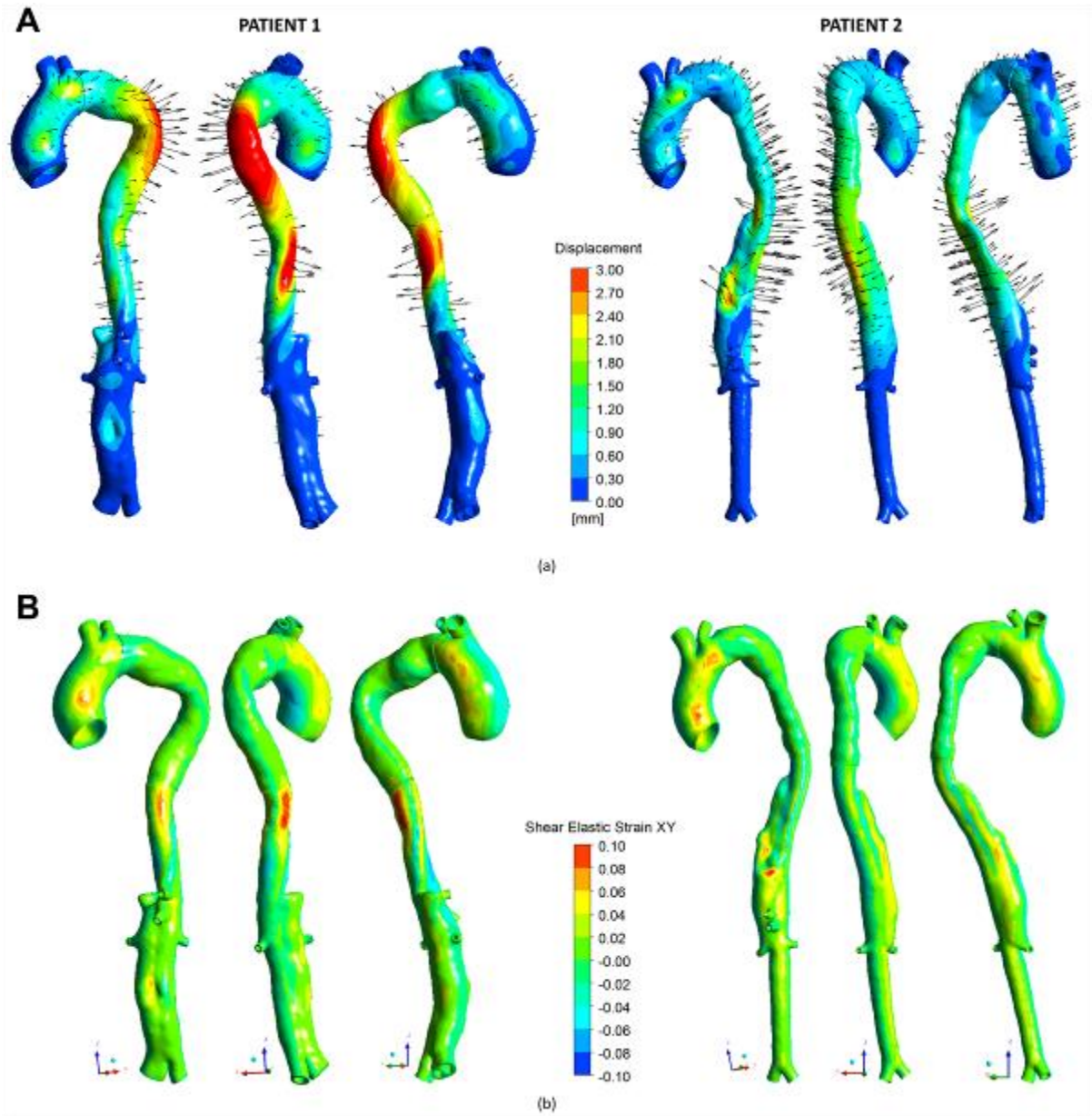


Figure 3. Stress distribution in Patients 1 and 2 obtained with the highest pressure load tested (50 mm Hg), corresponding to the pulse pressure in Patient 1. The red arrows show the locations of highest stress in each model. Regions A and B show the points of peak stress near the proximal and distal ends of the stent-graft.

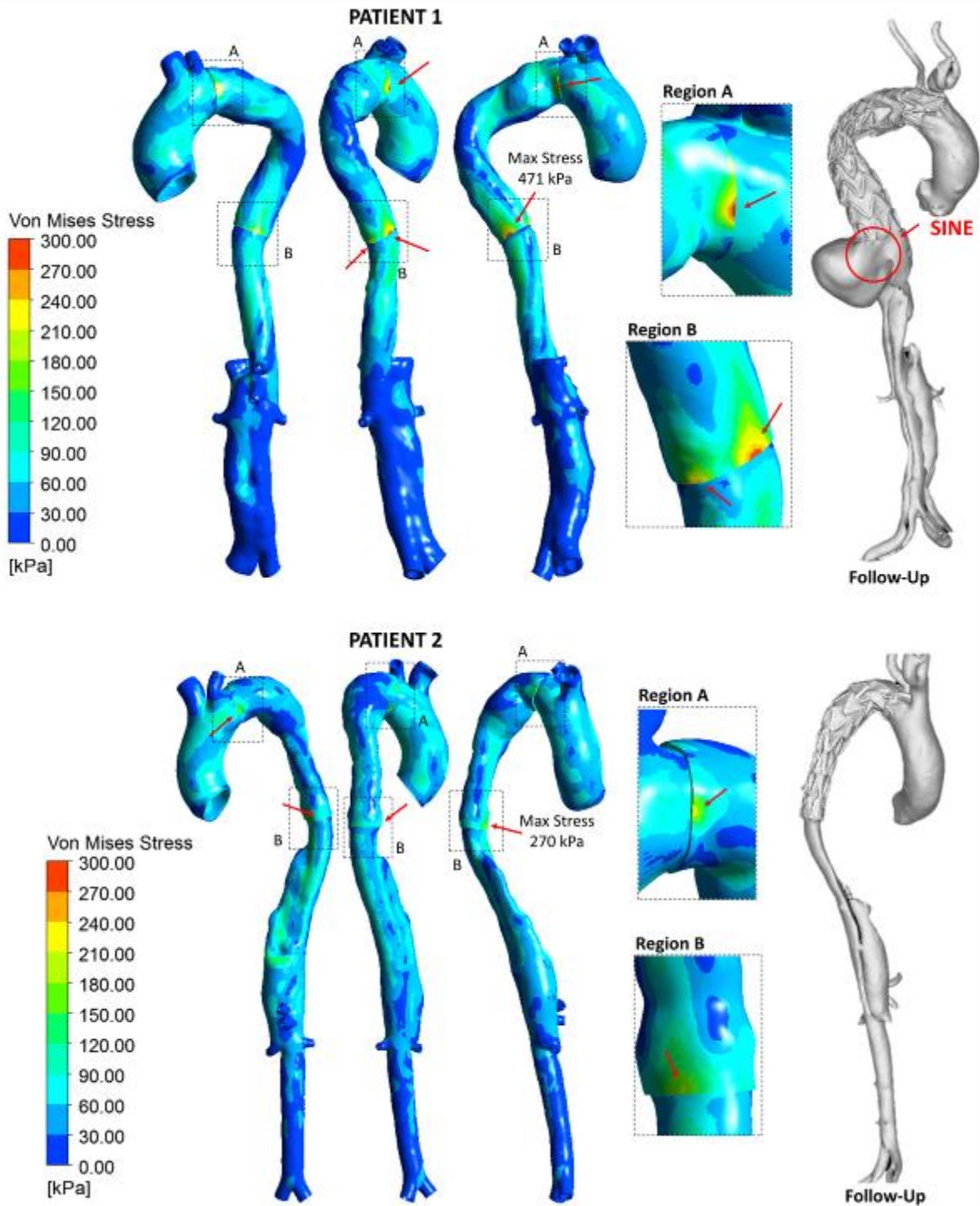


Table 1. Morphologic Measurements Taken From Computed Tomography Scans Acquired Before Thoracic Endovascular Aortic Repair and at the First Follow-up.

	Before TEVAR	3 Months Post TEVAR	Change, %
Patient 1			
TL volume, ^a mm ³	71855.3	99925.5	+39
FL volume, mm ³	270633.3	32008.1	-88
Ascending aorta diameter (d ₁), mm	34.0	34.0	0
Internal arch width (d ₂), mm	61.2	73.0	19
Descending aorta maximum diameter, mm	54.3	32.6	-40
Length of thoracic aorta, ^a mm	236.0	203.5	-14
Normalized length of thoracic aorta ^{a,b}	0.57	0.55	-4
Thoracic tortuosity index ^a	1.43	1.28	-10
Aortic tortuosity index ^a	1.43	1.16	-19
Stent tortuosity index	—	1.64	—
Thoracic region TL volume, ^a mm ³	37276.6	64963.6	+74
FL volume, mm ³	220248.9	0.00	-100
Abdominal region TL volume, ^a mm ³	34578.8	34961.9	+1
FL volume, mm ³	50384.4	32008.1	-36
Patient 2			
TL volume, ^a mm ³	54832.6	71407.4	+30
FL volume, mm ³	99483.5	20179.8	-80
Ascending aorta diameter (d ₁), mm	27.3	28.2	3
Internal arch width (d ₂), mm	37.2	57.9	56
Descending aorta maximum diameter, mm	36.4	30.2	-17
Length of thoracic aorta, ^a mm	195.4	179.9	-8
Normalized length of thoracic aorta ^{a,b}	0.52	0.48	-7
Thoracic tortuosity index ^a	1.19	1.16	-2
Aortic tortuosity index ^a	1.09	1.10	+1
Stent tortuosity index	—	1.28	—
Thoracic region TL volume, ^a mm ³	28439.6	43537.3	+53
FL volume, mm ³	75184.6	18679.2	-75
Abdominal region TL volume, ^a mm ³	26393.0	27870.1	+6
FL volume, mm ³	24298.9	1500.7	-94

Abbreviations: FL, false lumen; TEVAR, thoracic endovascular aortic repair; TL, true lumen.

^aMeasured from the root of the left subclavian artery.

^bNormalized against the total length of the descending aorta, measured from the root of the left subclavian artery up to the aortic bifurcation.